Chapter 12
Ternary Electrodes Under Equilibrium or Near-Equilibrium Conditions

12.1 Introduction

The previous chapter described binary electrodes, in which the microstructure is composed of phases made up of two elements. It was pointed out that there are also cases in which three elements are present, but only partial equilibrium can be obtained in experiments, so the electrode behaves as though it were composed of two, rather than three, components.

This chapter discusses active materials that contain three elements, but have kinetic behavior such that they behave as true ternary systems. As before, it will be seen that phase diagrams and equilibrium electrochemical titration curves are very useful thinking tools in understanding the potentials and capacities of electrodes containing such materials.

It is generally more difficult to obtain complete equilibrium in ternary systems than in binary systems, so that much of the available equilibrium, or near-equilibrium, information stems from experiments at elevated temperatures. Selective, or partial, equilibrium is much more common at ambient temperatures. This will be discussed in another chapter.

12.2 Ternary Phase Diagrams and Phase Stability Diagrams

In order to represent compositions in a three-component system one must have a figure that represents the concentrations of three components. This can be done by using a two-dimensional figure, as will be seen shortly. However, if information about the influence of temperature is also desired, a three-dimensional figure is required. This is often done in metallurgical and ceramic systems in which experiments commonly involve changes in the temperature. Most electrochemical
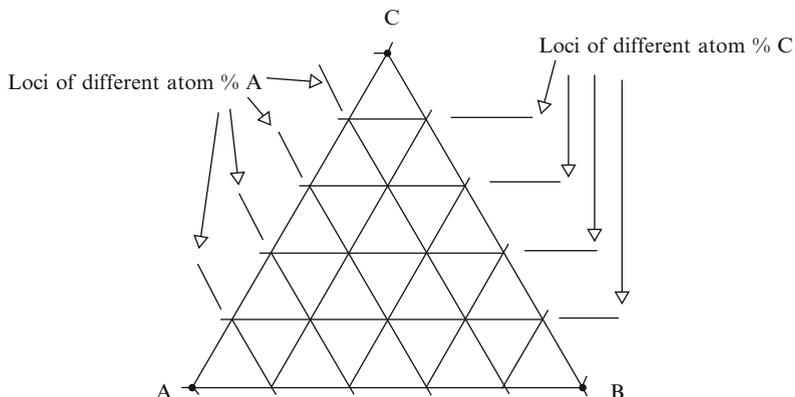
Fig. 12.1 General coordinate scheme used to depict compositions and phase equilibria in ternary systems on isothermal Gibbs triangles

systems operate at or near constant temperatures, so three-dimensional figures are not generally considered necessary.

Compositions in isothermal ternary systems can be represented on paper by using a triangular coordinate system. The method that is commonly employed in materials systems involves the use of *isothermal Gibbs triangles*. This scheme is illustrated in Fig. 12.1.

Compositions are expressed in terms of the atomic percent of each of the three components, indicated as A, B, and C in this case. For the purposes of this discussion it is desirable to have elements as components, so that three elements are placed at the corners, and the atomic percent of an element varies from zero along the opposite side to 100 % at its corner. Thus the position of each point within the triangle represents the atomic fraction of each of the elements present in the system.

Although phases in ternary systems often have ranges of composition, as they do in binary systems, it is often useful to simplify the phase equilibrium situation by assuming that they act as *point phases*. That is, that they have very narrow composition ranges. The term *phase stability diagram* will be used in this discussion to describe this approximation to the actual ternary phase diagram. It will be seen that it is possible to get a large amount of useful information by the use of such an approximate isothermal Gibbs triangle.

If there are phases inside the Gibbs triangle, the influence of the Gibbs phase rule must be considered. It was shown earlier that the Gibbs phase rule can be written as

$$F = C - P + 2 \tag{12.1}$$

If the temperature and total pressure are kept constant, the number of residual degrees of freedom F will be zero when there are three phases present in a ternary system. Three phases are in equilibrium with each other within triangles inside the overall Gibbs triangle. Two phases are in equilibrium if their compositions are
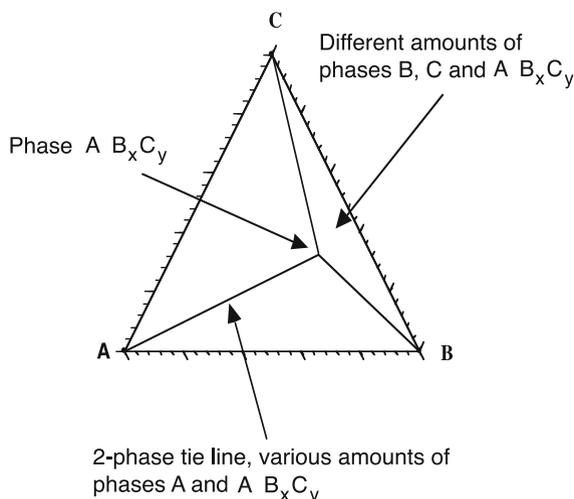
Fig. 12.2 Isothermal phase stability diagram ABC for the case in which there is a single intermediate phase whose composition is A_xB_yC

connected by a line, called a *two-phase tie line*. As shown in Fig. 12.2, if intermediate ternary phases are present, the total area within the Gibbs triangle is divided into *sub-triangles* whose sides are *two-phase tie lines*.

All of the compositions that lie within a given triangle have microstructures that are composed of mixtures of the three phases that are at the corners of that triangle. The overall composition determines the amounts of these different phases present, but not their compositions, for the latter are specified by the locations of the points at the corners of the relevant triangle. Any materials having compositions that fall along one of the sides of a triangle will have microstructures composed of the two phases at the ends of that tie line. The amounts are determined by the position of the composition along the tie line. Points closer to a given end have greater amounts of the phase whose composition is at the end.

Because the compositions of the phases present within triangles are constant, determined by the locations on the corner points, all of the intensive (amount-independent) thermodynamic parameters and properties are the same for all compositions inside the triangle. Important intensive properties include the chemical potentials and activities of each of the components, and the electrical potential.

12.3   Comments on the Influence of Sub-triangle Configurations in Ternary Systems

Binary systems can be changed to ternary systems by the addition of an additional element. As an example, consider a lithium-based binary system Li-M, in which the lithium composition can be varied. The addition of an additional element X
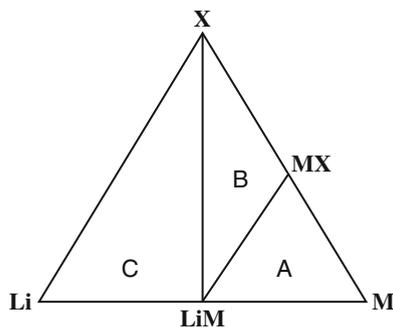
Fig. 12.3 Schematic ternary phase diagram for the Li-M-X system in which there are intermediate phases in the centers of both the Li-M and M-X binary systems

converts this to a ternary Li-M-X system. The presence of X can result in a significant change in the potentials in the Li-M system, even if X does not react with lithium itself.

Consider a simple case. Assume that the thermodynamic properties of this system lead to a ternary phase stability diagram of the type shown in Fig. 12.3, in which it is assumed that there are two stable binary phases, LiM, and MX.

If there is no X present, the composition moves along the Li-M edge of the ternary diagram, which is simply the binary Li-M system, and there will be a constant potential plateau for all compositions between pure M and LiM. The voltage vs. pure lithium in this compositional range, and therefore in triangle A of the ternary system, will be given by

$$E_A = \Delta G^\circ_f(\text{LiM})/F \tag{12.2}$$

What happens if lithium reacts with a material that has an original composition containing some X? The overall composition will follow a trajectory that starts at that position along the X-M side of the triangle and goes in the direction of the lithium corner of the ternary diagram. The addition of X to the M will not change the plateau potential for all compositions in triangle A. Therefore, there will be a plateau at that potential. Its length, however, will vary, depending upon the starting composition.

In addition, an additional plateau will appear at higher lithium concentrations as the overall composition enters and traverses triangle B. The potential of all compositions in that triangle will be given by

$$E_B = \left(\Delta G^\circ_f(\text{MX}) - \Delta G^\circ_f(\text{LiM})\right)/F \tag{12.3}$$

As in the case of the binary Li-M system, when the overall composition gets into triangle C the potential will be the same as that of pure lithium. These effects are illustrated in Figs. 12.4 and 12.5.

In Fig. 12.5 the variation of the electrode potential with overall composition is shown schematically for three different starting electrode compositions in Fig. 12.4.
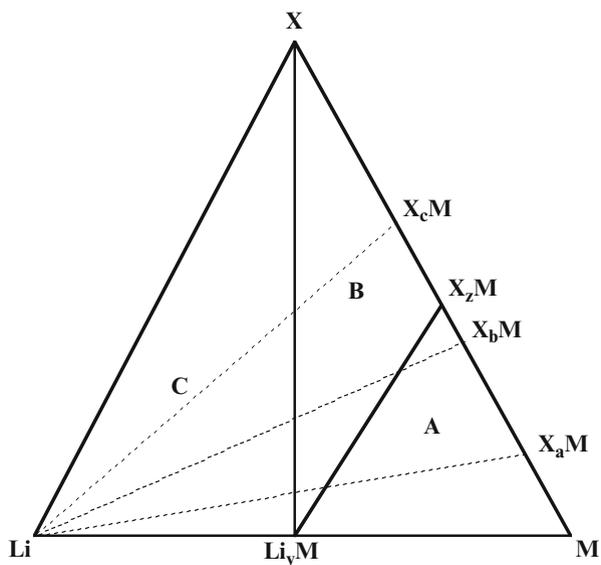
Fig. 12.4 The ternary Li-M-X system shown in Fig. 12.3, showing the loci of the overall composition for three different initial compositions
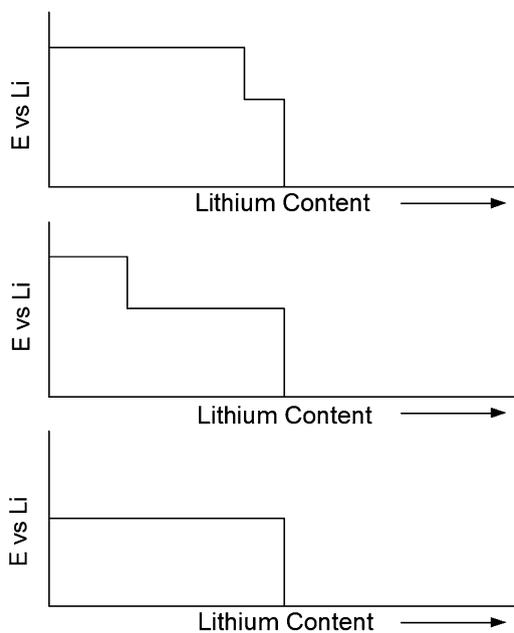

Fig. 12.5 Variation of the potential as lithium is added to electrodes with the three different starting compositions shown in Fig. 12.4. *Top*: X_aM, *middle*: X_bM, and *bottom*: X_cM
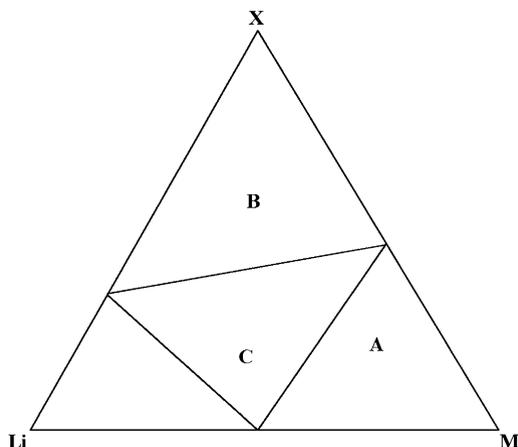
Fig. 12.6 Hypothetic ternary-phase diagram in which there is one intermediate phase in each of the binary systems

In all three cases, the number of moles of lithium stored per mole of M does not change, but the weight of the electrode will change, depending upon the relative weights of M and X. In addition, the average electrode potential becomes closer to that of pure lithium. This can be either advantageous or disadvantageous, depending upon whether the material is used as a negative electrode or as a positive electrode in a lithium-based cell.

Another ternary-phase configuration is shown in Fig. 12.6. In this case, it is assumed that there is also an intermediate phase in the Li-X binary system. The weight of the electrode per mol of Li will be reduced if the weight of Li_xX per mol of Li is less than that of Li per mol of Li_yM.

In practice, a binary system containing several intermediate phases may not be useful over its entire range of lithium composition, due to the change of the potential with composition. Poor diffusion kinetics in one of the intermediate phases or the terminal phase can also be deleterious.

There are many other possible phase diagram configurations in ternary systems, including those containing ternary phases in the interior of the diagram. In screening possible systems for study, however, a logical starting point is to examine systems with known binary and ternary phases.

12.4   An Example: The Sodium/Nickel Chloride "Zebra" System

Some years ago an interesting battery system suddenly appeared that had been initially developed in secret in South Africa and England. It is based upon the use of the solid electrolyte Na β-alumina, as in the Na/Na_xS system, which will be discussed later.

The β-alumina is a ceramic material that is a sodium-aluminum oxide with a nominal composition of $NaAl_{11}O_{17}$. It has a layer-type crystal structure in which the sodium ions have a very high mobility, so that it has the properties of a solid electrolyte.

This novel battery soon became known as the "*Zebra*" *cell* as the result of its development in South Africa.

It operates at 250–300 °C, and uses liquid sodium as the negative electrode, which is enclosed in a solid β-alumina tube. At this temperature sodium is liquid, and the ionic conductivity of the β-alumina is quite high. When the cell is fully charged, the positive electrode reactant is finely powdered $NiCl_2$, which is present adjacent to the β-alumina inside a solid container. Because the contact between the solid β-alumina tube and the particles of $NiCl_2$ is only at their points of contact, a second (liquid) electrolyte, $NaAlCl_4$, is also present in the outer, positive electrode compartment, part of the cell. Thus the full surface area of the $NiCl_2$ particles acts as the electrochemical interface, which greatly increases the kinetics.

Thus this electrochemical system, when charged, has the configuration:

$$Na/Na\ \beta-alumina/NaAlCl_4/NiCl_2$$

The physical arrangement of this cell is shown schematically in Fig. 12.7.

The electrochemical behavior of a Zebra cell can be understood by consideration of the Na-Ni-Cl ternary phase diagram. Thermodynamic data indicate that there are only two binary phases in this ternary system, $LiCl_2$, and NaCl. They lie on two different sides of the ternary Na-Ni-Cl-phase diagram. Since the total area must be
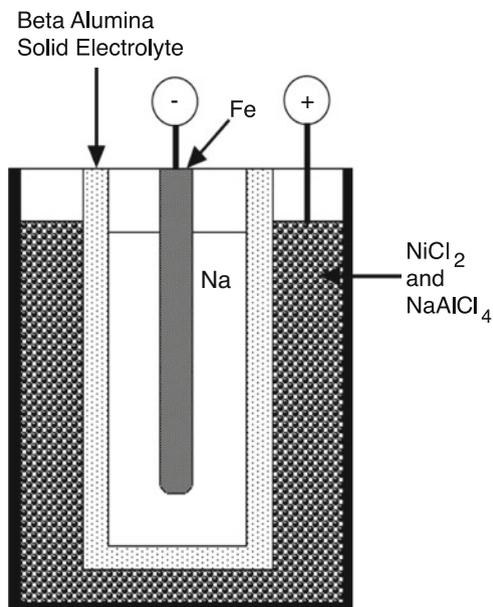

Fig. 12.7 Schematic view of the "Zebra" cell, which operates at 250–300 °C
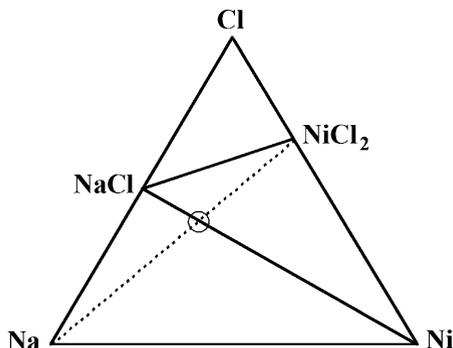
Fig. 12.8 The Na-Ni-Cl ternary phase diagram, showing the locus of the overall composition as Na reacts with $NiCl_2$

divided into triangles, it is evident that there are two possibilities. There is either a tie line from $NiCl_2$ to the Na corner, or there is one from NaCl to the Ni corner. The decision as to which of these is stable can be determined by the direction of the virtual reaction

$$2Na + NiCl_2 = 2NaCl + Ni \qquad (12.4)$$

The Gibbs free energy change in this virtual reaction is given by

$$\Delta G_r^\circ = 2\Delta G_f^\circ(NaCl) - \Delta G_f^\circ(NiCl_2) \qquad (12.5)$$

Values of the standard Gibbs free energies at 275 °C of NaCl and $NiCl_2$ are -360.25 kJ/mol and -221.12 kJ/mol, respectively. Therefore the reaction in Eq. (12.4) will tend to go to the right, and the tie line between NaCl and Ni is more stable than the one between $NiCl_2$ and Na.

As a result, the phase stability diagram must be as shown by the solid lines in Fig. 12.8. As Na reacts with $NiCl_2$ the overall composition of the positive electrode follows the dotted line in that figure. When it reaches the composition indicated by the small circle, all of the $NiCl_2$ will have been consumed, and only NaCl and Ni are present.

So long as the overall composition remains in the $NaCl\text{-}NiCl_2\text{-}Ni$ triangle, the potential is constant. Its value can be calculated from the Gibbs free energy of reaction value corresponding to Eq. (12.5). The voltage of the positive electrode with respect to the pure Na negative electrode is given by

$$\Delta E = -\Delta G_r^\circ / zF \qquad (12.6)$$

where $z = 2$, according to the reaction is Eq. (12.4). The result is that the potential of all compositions within that triangle in the ternary diagram, and also across the Zebra cell, is constant, and equal to 2.59 V. This is also what is observed experimentally.

12.5   A Second Example: The Lithium-Copper-Chlorine Ternary System

The Li-Cu-Cl system will be used as a further example to illustrate these principles, and show how useful information can be derived from a combination of a ternary phase diagram and thermodynamic data related to the stable phases within it.

Thermodynamic information shows that there are three stable phases within this system at 298 K, LiCl, CuCl, and $CuCl_2$. Values of their standard Gibbs free energies of formation are given in Table 12.1.

All of these phases lie on the edges of the isothermal Gibbs triangle. If they are assumed to be point phases, with negligible ranges of composition, the phase stability diagram can be constructed by following a few simple rules and procedures.

1. The total area must be divided into triangles. Their edges are tie lines between pairs of phases.
2. No more than three phases can be present within a triangle. Their compositions must be at the corners.
3. Tie lines cannot cross.

The first task is to determine the stable tie lines in this system. This can be done by drawing all the possible tie lines between the stable phases on a trial basis, and then determining which of them are stable. The end result must be that the overall triangle is divided into sub-triangles.

The line between LiCl and $CuCl_2$ must be stable, as there are no other possible lines that could cross it. There are four additional possibilities, lines between Li and $CuCl_2$, Li and CuCl, LiCl and CuCl, and Li and Cu. A method that can be used to determine which of these is actually stable is to write the virtual reactions between the phases at the ends of conflicting (crossing) tie lines. Which of the two pairs of phases are more stable in each case can be determined from the available thermodynamic data.

As an example, consider whether there is a tie line between LiCl and Cu or one between CuCl and Li. Both cannot be stable, for they would cross.

The virtual reaction between the pairs of possible end phases can be written as

$$LiCl + Cu = CuCl + Li \tag{12.7}$$

Table 12.1 Gibbs free energies of formation of phases in the Li-Cu-Cl system

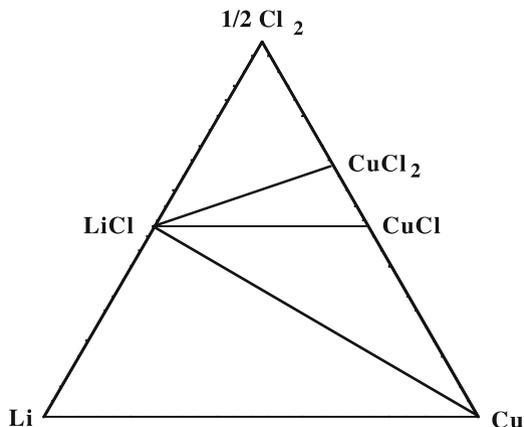| Phase	ΔG_f° at 298 K (kJ/mol)
LiCl	−384.0
CuCl	−138.7
$CuCl_2$	−173.8

Fig. 12.9 Isothermal phase stability diagram for the Li-Cu-Cl ternary system at 25 °C

As before, the direction in which this virtual reaction would tend to go can be determined from the value of the standard Gibbs free energy of reaction. In this case, it is given by

$$\Delta G_r^\circ = \Delta G_f^\circ(CuCl) - \Delta G_f^\circ(LiCl) \tag{12.8}$$

The result is that ΔG_r° is $(-138.7) - (-384.0) = +245.3$ kJ/mol. Thus this reaction would tend to go to the left. This means that the combination of the phases LiCl and Cu is more stable than the combination of CuCl and Li. Thus the tie line between LiCl and Cu is stable in the phase diagram.

This implies that the tie line between LiCl and Cu is also more stable than one between $CuCl_2$ and Li, and also that a line between LiCl and CuCl exists. These conclusions can be verified by consideration of the virtual reaction between LiCl and Cu, and $CuCl_2$ and Li. This reaction would be written as

$$2LiCl + Cu = CuCl_2 + 2Li \tag{12.9}$$

for which the standard Gibbs free energy of reaction is $(-173.8) - 2(-384.0) = +594.2$ kJ/mol. Thus these conclusions were correct.

The resulting isothermal phase stability diagram for this system is shown in Fig. 12.9.

12.5.1 Calculation of the Voltages in this System

From this diagram and the thermodynamic data the voltages and capacities of electrodes in this system can also be calculated. As the first example, consider the
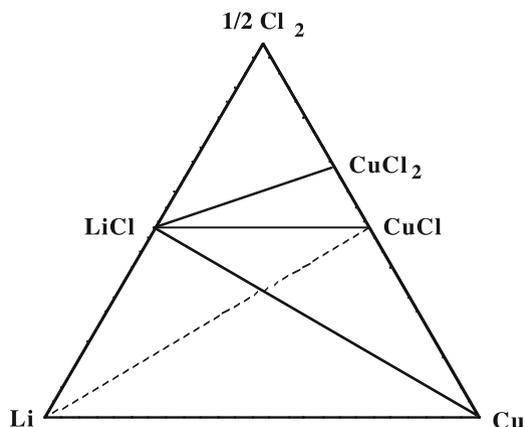
Fig. 12.10 Use of ternary phase diagram to understand the reaction of lithium with CuCl

reaction of lithium with CuCl. This reaction can be understood in terms of the ternary phase diagram as shown in Fig. 12.9.

By the addition of lithium the overall composition moves from the initial composition at the CuCl point along the dotted line toward the Li corner, as shown in Fig. 12.10. In doing so, it moves into and across the LiCl–CuCl–Cu triangle. So long as it is inside this triangle its voltage remains constant.

This voltage can be calculated from the virtual reaction that takes place by the addition of lithium as the overall composition moves into, and through, the LiCl-CuCl-Cu triangle:

$$Li + CuCl = LiCl + Cu \qquad (12.10)$$

The standard Gibbs free energy change as the result of this reaction is $(-384.0) - (-138.7) = -245.3$ kJ/mol. The voltage can be calculated from

$$E = -(-245.3)/[(1)(96.5)] \qquad (12.11)$$

The result is 2.54 V vs. pure Li. This voltage remains constant as long as the overall composition stays in the LiCl-CuCl-Cu triangle. It is obvious from Eq. (12.10) and the phase diagram in Fig. 12.10 that up to 1 mol of Li can participate in this reaction. Thus the equilibrium titration curve, the variation of the voltage of a cell of this type as a function of composition can be drawn as in Fig. 12.11.

If, on the other hand, the positive electrode were to consist of $CuCl_2$ instead of CuCl, the overall composition would move along the dotted line shown in Fig. 12.12.

The overall composition first enters the LiCl-CuCl$_2$-CuCl triangle. The relevant virtual reaction for this triangle is
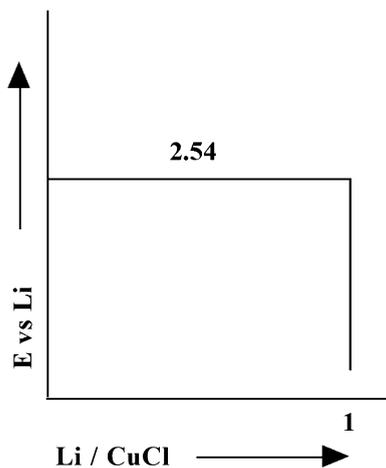
Fig. 12.11 Variation of the equilibrium voltage of Li/CuCl cell as a function of the extent of reaction
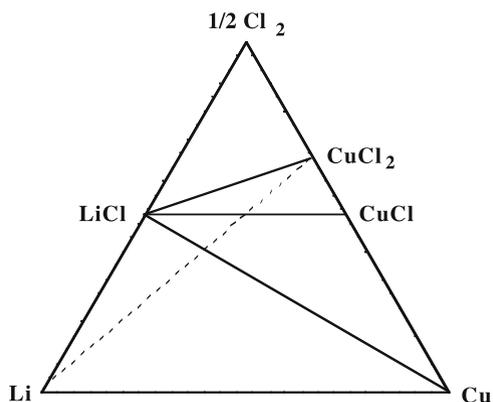

Fig. 12.12 Use of ternary phase stability diagram to understand the reaction of Li with $CuCl_2$

$$Li + CuCl_2 = LiCl + CuCl \tag{12.12}$$

The standard Gibbs free energy change as the result of this reaction is (-384.0) $+(-138.7) - (-173.8) = -348.9$ kJ/mol. The voltage with respect to pure Li can be calculated from

$$E = -\Delta G_r^\circ /zF = 348.9/96.5 \tag{12.13}$$
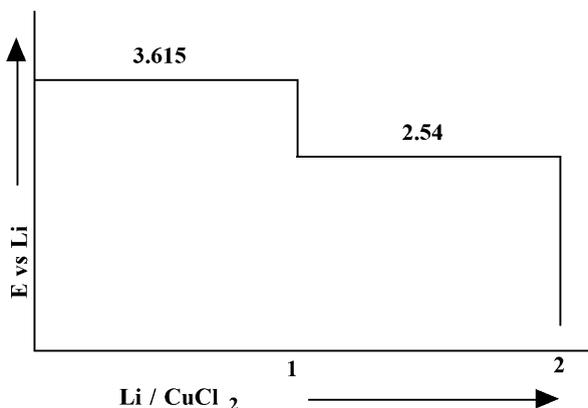
or 3.615 V vs. Li

Fig. 12.13 Equilibrium titration curve for the reaction of lithium with $CuCl_2$ to form LiCl and CuCl, and then more LiCl and Cu

There will be a plateau at this voltage in the equilibrium titration curve. The LiCl cannot react further with Li. But the CuCl that is formed in this reaction can undergo a further reaction with additional lithium. When this happens the overall composition moves into and across the second triangle, whose corners are at LiCl, CuCl and Cu. Although the reaction path is different, this is the same triangle whose voltage was calculated above for the reaction of lithium with CuCl. Thus the same voltage will be observed, 2.54 V vs. Li, in this second reaction, written in Eq. (12.10). The equilibrium titration curve will therefore have two plateaus, related to the two triangles that the overall composition traverses as lithium reacts with $CuCl_2$. This is shown in Fig. 12.13.

12.5.2   *Experimental Arrangement for Lithium/Copper Chloride Cells*

Cells based upon the reaction of lithium with either of the copper chloride phases can be constructed at ambient temperature using an electrolyte with a nonaqueous solvent, such as propylene carbonate, containing a lithium salt such as $LiClO_4$. There are a number of alternative solvents, as well as alternative salts, and this topic will be discussed in a later chapter. The important thing at the present time is that water and oxygen must be avoided, and the salt should have a relatively high solubility in the nonaqueous solvent.

12.6   Calculation of the Maximum Theoretical Specific Energies of Li/CuCl and Li/CuCl$_2$ Cells

The maximum values of specific energies that might be obtained from electro-chemical cells containing either CuCl or CuCl$_2$ as positive electrode reactants can be calculated from this information.

As shown in an earlier chapter, the general relation for the maximum theoretical specific energy (MTSE) is

$$MTSE = (xV/W)(F) \text{ kJ/kg} \tag{12.14}$$

where x is the number of mols of Li involved in the reaction, V the average voltage, and W the sum of the atomic weights of the reactants. F is the Faraday constant, 96,500 C/mol.

In the case of a positive electrode that starts as CuCl and undergoes reaction (12.10), the sum of the atomic weights of the reactants is $(7 + 63.55 + 35.45) = 106.0$ g. The value of x is unity, and the average cell voltage is 2.54 V. Thus the MTSE is 2312.4 kJ/kg.

This can be converted to Wh/kg by dividing by 3.6, the number of kJ per Wh. The result is that the MTSE can be written as 642.3 Wh/kg for this reaction.

If the positive electrode starts as CuCl$_2$ and undergoes reaction (12.12) to form LiCl and CuCl the weight of the reactants is $(7 + 63.55 + (2 \times 35.45)) = 141.45$ g. The value of x is again unity, and the cell voltage was calculated to be 3.615 V. This then gives a value of MTSE of 2466.2 kJ/kg. Alternatively, it could be expressed as 685.1 Wh/kg.

If further lithium reacts with the products of this reaction, the voltage will proceed along the lower plateau, as was the case for an electrode whose composition started as CuCl. Thus additional energy is available. However, the total specific energy is not simply the sum of the specific energies that have just been calculated for the two plateau reactions independently. The reason for this is that the weight that must be considered in the calculation for the second reaction is the starting weight before the first reaction in this case.

Then, for the second plateau reaction:

$$MTSE = (1)(2.54)(96,500)/141.45 = 1732.8 \text{ kJ/kg} \tag{12.15}$$

This is less than for the second plateau alone, starting with CuCl, which was shown above to be 2312 kJ/kg. Alternatively, the specific energy content of the second plateau for an electrode that starts as CuCl$_2$ is 481.3 Wh/kg instead of 642.3 Wh/kg, if it were to start as CuCl.

Thus if the electrode starts out as CuCl$_2$, the total MTSE can be written as

$$MTSE = 2466.2 + 1732.8 = 4199 \text{ kJ/kg} \tag{12.16}$$

Or alternatively, $685.1 + 481.3 = 1166.4$ Wh/kg.

12.7   Specific Capacity and Capacity Density in Ternary Systems

As mentioned earlier, other parameters that are often important in battery systems are the capacity per unit weight or per unit volume. In the case of ternary systems, the capacity along a constant potential plateau is determined by the length of the path of the overall composition within the corresponding triangle. This is determined by the distance along the composition line between the binary tie lines at the boundaries of the triangles.

12.8   Another Group of Examples: Metal Hydride Systems Containing Magnesium

Binary alloys are often used as negative electrodes in hydrogen-transporting electrochemical cells. When they absorb or react with hydrogen, they are generally called *metal hydrides*. Because of the presence of hydrogen as well as the two metal components, they become ternary systems.

There is a great interest in the storage of hydrogen for a number of purposes related to the desire to reduce the dependence on petroleum. The reversible hydrogen absorption in some metal hydrides is a serious competitor for this purpose.

If the kinetics of hydrogen absorption or reaction are relatively fast, and the motion of the other constituents in the crystal structure is very sluggish, so that no structural reconstitution of the metal constituents in the microstructure takes place in the time scale of interest, such metal hydride systems can be treated as *pseudo-binary systems*, i.e., hydrogen plus the metal alloy. This is the general assumption that is almost always found in the literature on the behavior of metal hydrides.

On the other hand, there are materials in which this is not the case, and the hydrogen-metal hydride combination should be treated as a ternary system. Experiments have shown that the reaction of hydrogen with several binary magnesium alloys provides examples of such ternary systems [1, 2].

The prior examples of the reaction of lithium with the two copper chloride phases were used to illustrate how thermodynamic information can be used to determine the phase diagram and the electrochemical properties. These hydrogen/magnesium-alloy systems will be discussed, however, *as reverse examples*, in which electrochemical methods can be used in order to determine the relevant phase diagrams and thermodynamic properties, as well as to determine the practical parameters of energy and capacity.

Metal hydride systems are typically studied by the use of gas absorption experiments, in which the hydrogen pressure and temperature are the primary external variables. Electrochemical methods can generally also be employed by the use of a suitable electrolyte and cell configuration. Variation of the cell voltage

can cause a change in the difference between the effective hydrogen pressure in the two electrodes. If one electrode has a fixed hydrogen activity, the hydrogen activity in the other can be varied by the use of an applied voltage. This then causes either the absorption or desorption of hydrogen. This can be expressed by the Nernst relation:

$$E = (RT/zF)\Delta \ln p(\text{H}_2) \tag{12.17}$$

where E is the cell voltage, R the gas constant, T the absolute temperature, z the charge carried by the transporting ion (hydrogen), and F the Faraday constant. The term $\Delta \ln p(\text{H}_2)$ is the difference in the natural logarithms of the effective partial pressures, or activities, of hydrogen at the two electrodes.

Electrochemical methods can have several advantages over the traditional pressure-temperature methods. Since no temperature change is necessary for the absorption or desorption, data can be obtained at a constant temperature. If a stable reference is used, variation of the cell voltage determines the hydrogen activity at the surface of the alloy electrode. Large changes in hydrogen activity can be obtained by the use of relatively small differences in cell voltage. Thus the effective pressure can be easily and rapidly changed over several orders of magnitude. The amount of hydrogen added to, or deleted from, an electrode can be readily determined from the amount of current that passes through the cell.

One of the important parameters in the selection of materials for hydrogen storage is the amount of hydrogen that can be stored per unit weight of host material, the specific capacity. This is often expressed as the ratio of the weight of hydrogen absorbed to the weight of the host material. Magnesium-based hydrides are considered to be potentially very favorable in this regard, for the atomic weight of magnesium is quite low, 24.3 g per mol. MgH_2 contains 1 mol of H_2, and the ratio 2/24.3 means 8.23 w/% hydrogen. This can be readily converted to the amount of charge stored per unit weight, i.e. the number of mAh/g. One Faraday is 96,500 C, or 26,800 mAh, per equivalent. The addition of two hydrogens per magnesium means that two equivalents are involved. Thus 2204 mAh of hydrogen can be reacted per gram of magnesium.

On the other hand, one is often interested in the amount of hydrogen that can be obtained by the decomposition of a metal hydride. This means that the weight to be considered is that of the metal plus the hydrogen, rather than just the metal itself. When this is done, it is found that 7.6 w/%, or 2038 mAh/g hydrogen can be obtained from MgH_2.

These values for magnesium hydride are over five times those of the materials that are commonly used as metal hydride electrodes in commercial battery systems. Thus there is continued interest in the possibility of the development of useful alloys based upon magnesium. The practical problem is that magnesium forms a very stable oxide, which acts as a barrier to the passage of hydrogen. It is very difficult to prevent the formation of this oxide on the alloy surface in contact with the aqueous electrolytes commonly used in battery systems containing metal hydrides.
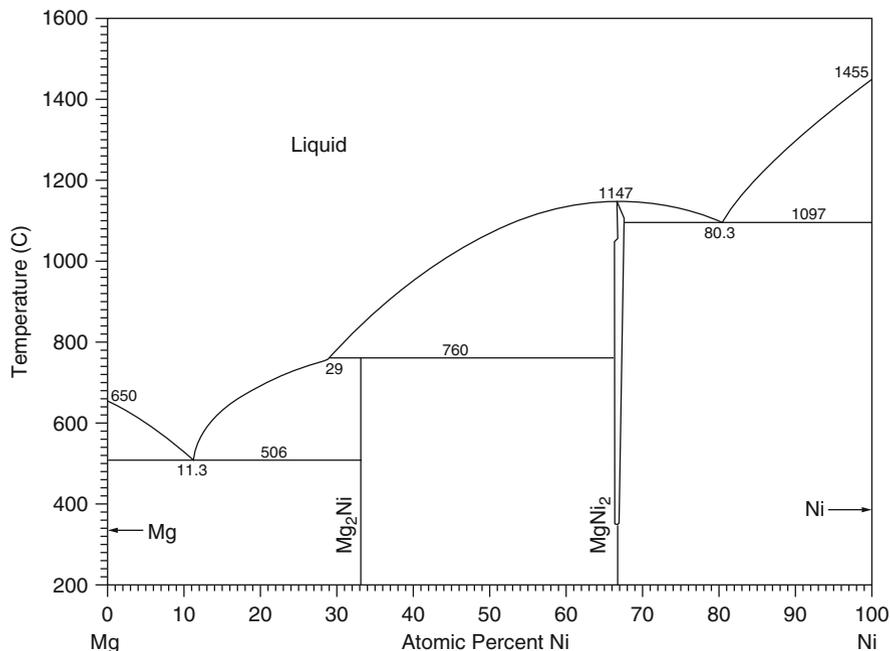
Fig. 12.14 Magnesium–nickel binary phase diagram

One of the strategies that have been explored is to put a material such as nickel, which is stable in these electrolytes, on the surface of the magnesium. It is known that nickel acts as a mixed conductor, allowing the passage of hydrogen into the interior of the alloy. However, this surface covering cannot be maintained over many charge/discharge cycles, with the accompanying volume changes.

A different approach is to use an electrolyte in which magnesium is stable, but its oxide is not. This was demonstrated by the use of a novel intermediate temperature alkali organo-aluminate molten salt electrolyte $NaAlEt_4$ [1]. The hydride salt NaH can be dissolved into this melt, providing hydride ions, H^-, that can transport hydrogen across the cell. This salt is stable in the presence of pure Na, which can then be used as a reference, as well as a counter, electrode.

This experimental method was used to study hydrogen storage in three ternary systems involving magnesium alloys, the H-Mg-Ni, H-Mg-Cu and H-Mg-Al systems. In order to be above the melting point of this organic anion electrolyte, these experiments were performed somewhat above 140 °C.

The magnesium-nickel binary phase diagram is shown in Fig. 12.14. It shows that there are two intermediate phases, Mg_2Ni and $MgNi_2$. It is also known that magnesium forms the dihydride MgH_2. These compositions are shown on the H-Mg-Ni ternary diagram shown in Fig. 12.15. Note that the ternary diagram is drawn with hydrogen at the top in this case.

In order to explore this ternary system, an electrochemical cell was used to investigate the reaction of hydrogen with three compositions in the Mg-Ni binary
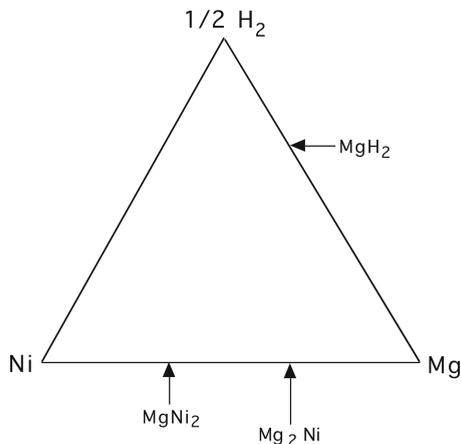
Fig. 12.15 The H-Mg-Ni ternary diagram showing only the known compositions along the binary edges
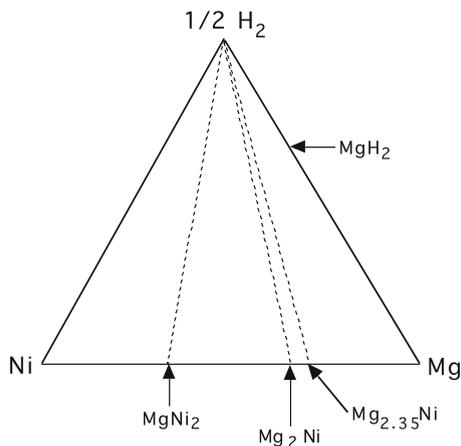

Fig. 12.16 Loci of the overall composition as hydrogen reacts with three initial Mg-Ni alloy compositions

alloy system, $MgNi_2$, Mg_2Ni, and $Mg_{2.35}Ni$. Thus the overall compositions of these materials moved along the dashed lines shown in Fig. 12.16 as hydrogen was added.

It was found that the voltage went to zero as soon as hydrogen was added to the phase $MgNi_2$. However, in the other cases, it changed suddenly from one plateau potential to another as certain compositions were reached. These transition compositions are indicated by the circles in Fig. 12.17. The values of the voltage versus the hydrogen potential in the different compositions regions are also shown in that figure.
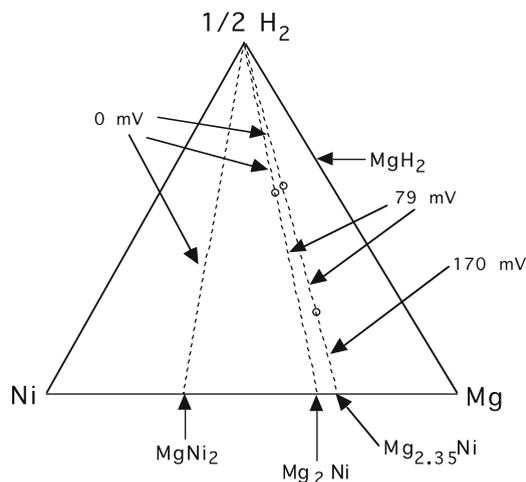
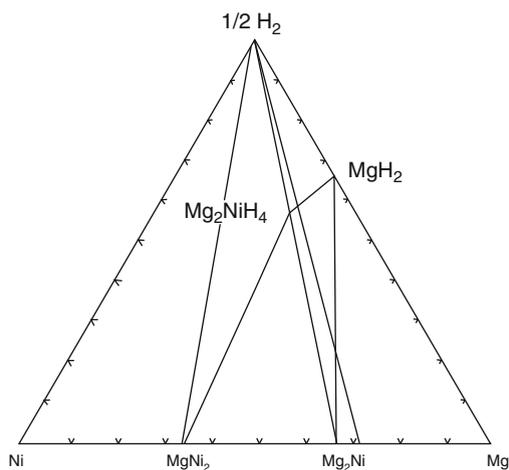**Fig. 12.17** Plateau voltages found in different composition regions

Fig. 12.18 Ternary phase stability diagram for the H-Mg-Ni system at about 140 °C, derived from the compositional variation of the potential as hydrogen was reacted with three different initial binary alloy compositions

This information can be used to construct the ternary equilibrium diagram for this system. As described earlier, constant potential plateaus are found for compositions in three-phase triangles, and potential jumps occur when the composition crosses two-phase tie lines. The result is that there are no phases between $MgNi_2$ and pure hydrogen, but there must be a ternary phase with the composition Mg_2NiH_4. The resulting H-Mg-Ni ternary diagram at this temperature is shown in Fig. 12.18.
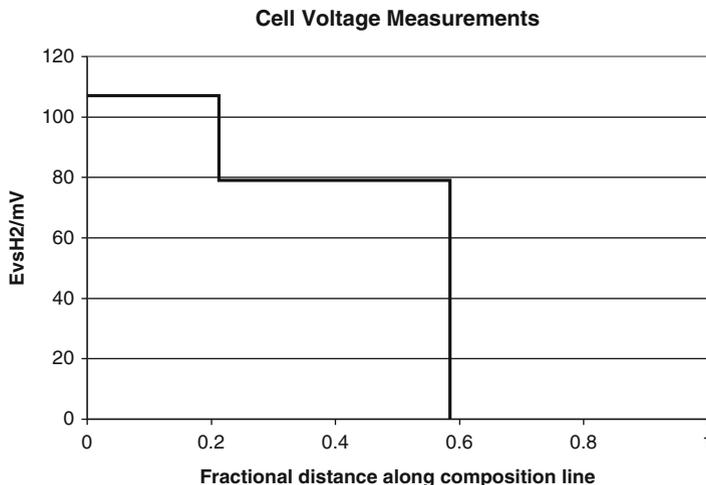
Cell Voltage Measurements

Fig. 12.19 Variation of the potential as hydrogen is added to alloy with an initial composition $Mg_{2.35}Ni$

The phase Mg_2Ni reacts with four hydrogen atoms to form Mg_2NiH_4 at a constant potential of 79 mV versus pure hydrogen. The weight of the Mg_2Ni host is 107.33 g, which is 26.83 g per mol of hydrogen atoms. This amounts to 3.73 % hydrogen atoms stored per unit weight of the initial alloy. This is quite attractive, and is considerably more than the specific capacity of the materials that are currently used in the negative electrodes of metal hydride/nickel batteries.

On the other hand, pure magnesium reacts to form MgH_2 at a constant potential of 107 mV versus pure hydrogen. Because of the lighter weight of magnesium than nickel, this amounts to 8.23 % hydrogen atoms per unit weight of the initial magnesium, or 7.6 w% relative to MgH_2. Thus the use of magnesium, and its conversion to MgH_2, is very attractive for hydrogen storage. There is a practical problem, however, due to the great sensitivity of magnesium to the presence of even small amounts of oxygen or water vapor in its environment.

If the initial composition is between Mg_2Ni and Mg, as is the case for the composition $Mg_{2.35}Ni$ that has been discussed above, there will be two potential plateaus, and their respective lengths, as well as the total amount of hydrogen stored per unit weight of the electrode, will have intermediate values, varying with the initial composition. As an example, the variation of the potential with the amount of hydrogen added to the $Mg_{2.35}Ni$ is shown in Fig. 12.19.

Similar experiments were carried out on the reaction of hydrogen with two other magnesium alloy systems, the H-Mg-Cu and H-Mg-Al systems [1]. Their ternary equilibrium diagrams were determined by using analogous methods. They are shown in Figs. 12.20 and 12.21.
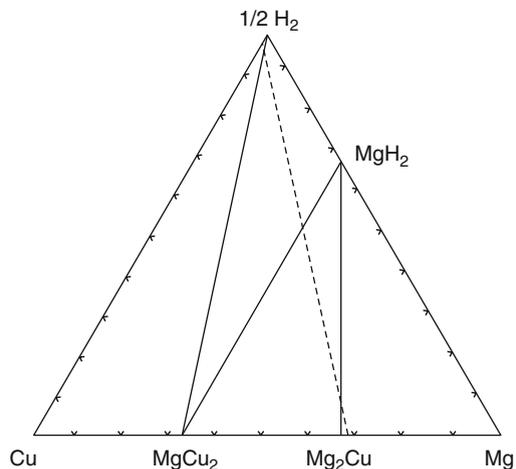
Fig. 12.20 Ternary phase stability diagram for the H-Mg-Cu system at about 140 °C, derived from the compositional variation of the potential as hydrogen was reacted with different initial binary alloy compositions using organic anion molten salt electrolyte
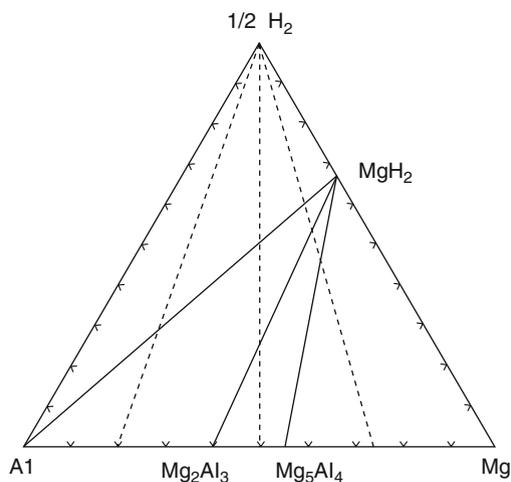

Fig. 12.21 Ternary phase stability diagram for the H-Mg-Al system at about 140 °C, derived from the compositional variation of the potential as hydrogen was reacted with different initial binary alloy compositions using organic anion molten salt electrolyte

12.9 Further Ternary Examples: Lithium-Transition Metal Oxides

These same concepts and techniques have been used to investigate several lithium-transition metal oxide systems [3, 4]. They will be discussed briefly here. These examples are different from those that have been discussed thus far, for in a number of cases the initial compositions are, themselves, ternary phases, not just binary phases.

They further illustrate how electrochemical measurements on selected compositions can be used to determine the relevant phase diagrams. This makes it possible to predict the potentials and capacities of other materials within the same ternary system without having to measure them individually.

In addition, it will be seen that one can obtain a correlation between the activity of lithium, and thus the potential, and the equilibrium oxygen partial pressure, of phases and phase combinations in some cases. This provides the opportunity to predict the potentials of a number of binary and ternary materials with respect to lithium from information on the properties of relevant oxide phases alone.

Data on the ternary lithium–transition metal oxide systems that will be presented here were obtained by the use of the LiCl–KCl eutectic molten salt as electrolyte at about 400 °C. They were studied at a time when there was a significant effort in the USA to develop large-scale batteries for vehicle propulsion using lithium alloys in the negative electrode and iron sulfide phases in the positive electrode. The transition metal oxides were being considered as alternatives to the sulfides.

Experiments employing this molten salt electrolyte system required the use of glove boxes that maintained both the oxygen and nitrogen concentrations at very low levels. This salt could be used for experiments to very negative potentials, limited by the evaporation of potassium. The maximum oxygen pressure that can be tolerated is limited by the formation of Li_2O. This occurs at a partial pressure of 10^{-15} atm at 400 °C. This is equivalent to 1.82 V versus lithium at that temperature. As a result, this electrolyte can not be used to investigate materials whose potentials are above 1.82 V relative to that of pure lithium. As will be seen later, many of the positive electrode materials that are of interest today operate at potentials above this limit.

The first example is the lithium-cobalt oxide ternary system. Experiments were made in which lithium was added to both the binary phase CoO and the ternary phase $LiCoO_2$. The variations of the observed equilibrium potentials as lithium was added to these phases are indicated in Fig. 12.22. It is seen that there were sudden drops from 1.807 to 1.636 V, and then to zero in the case of CoO. Starting with $LiCoO_2$, however, only one voltage jump was observed, from 1.636 to 0. Since these jumps occur when the composition crosses binary tie lines in such diagrams, it was very easy to plot the ternary figure in this case. The result is shown in Fig. 12.23, in which the values of the potential (voltage versus pure lithium), lithium activity, cobalt activity and oxygen partial pressure for the two relevant compositional triangles are indicated. As mentioned earlier, it was not possible to
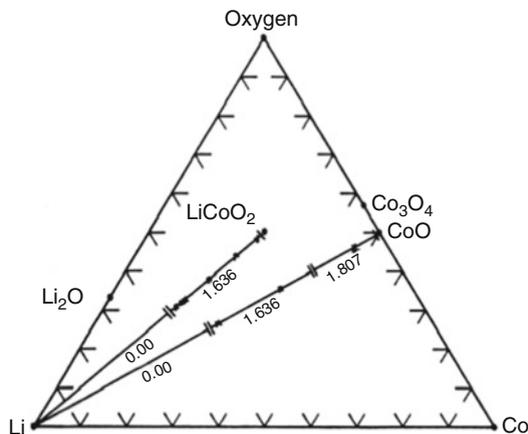
Fig. 12.22 Results of coulometric titration experiments on two compositions in the lithium-cobalt oxide system. After [4]
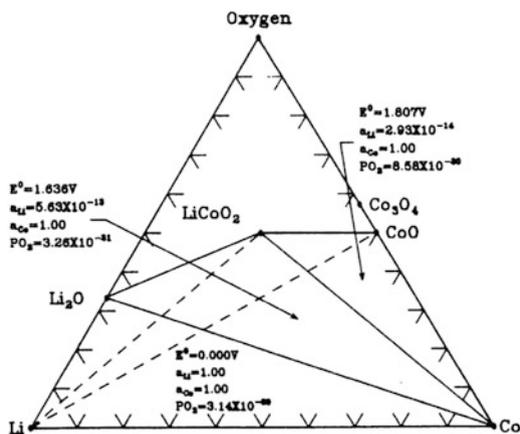

Fig. 12.23 Ternary phase stability diagram derived from the coulometric titration experiments shown in Fig. 12.22. After [4]

investigate the higher potential regions that are being used in positive electrodes today.

A further example is the Li-Fe-O system. Fig. 12.24 shows the variation of the equilibrium potential as lithium was added to Fe_3O_4 under near-equilibrium conditions. It is seen that this is a more complex case, for after a small initial solid solution region there are three jumps in the potential.

Similar experiments were undertaken on materials with two other initial compositions, $LiFe_5O_8$ and $LiFeO_2$. From these data it was possible to plot out the whole ternary system within the accessible potential range, as shown in Fig. 12.25.
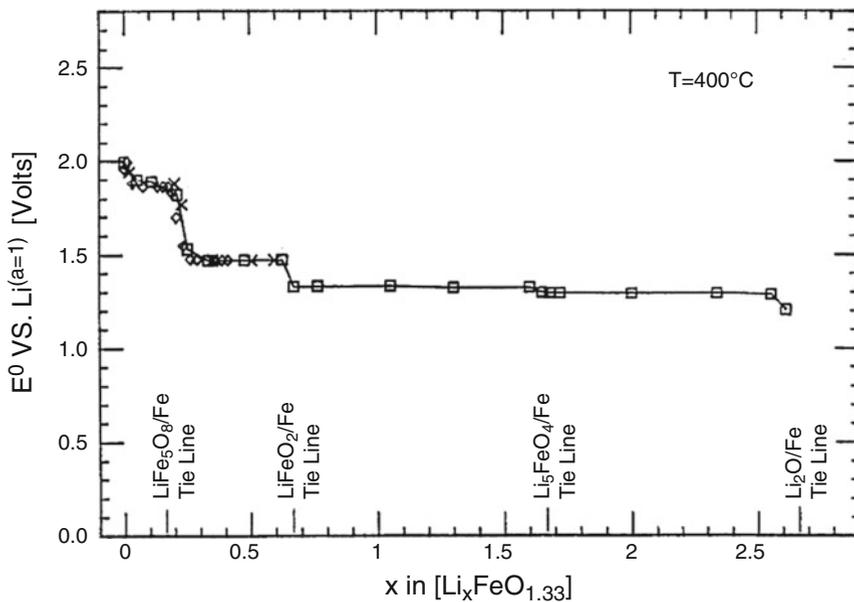
Fig. 12.24 Results of a coulometric titration experiment on a sample with an initial composition Fe_3O_4. After [4]
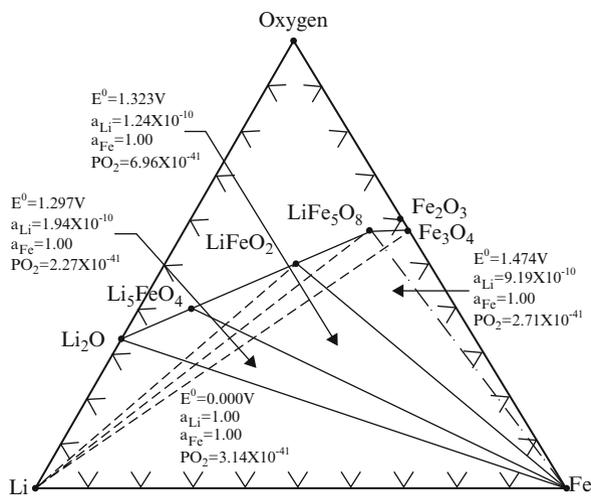

Fig. 12.25 Ternary phase stability diagram derived from coulometric titration measurements on materials in the Li-Fe-O ternary system. After [4]

Investigation of the Li-Mn-O system produced results that were somewhat different from those in the Li-Co-O and Li-Fe-O systems. The variation of the potential as lithium was added to samples with initial compositions MnO, Mn_3O_4, $LiMnO_2$ and Li_2MnO_3 is shown in Fig. 12.26. The ternary equilibrium diagram that resulted in shown in Fig. 12.27. It is seen that all of the two-phase tie lines do not go
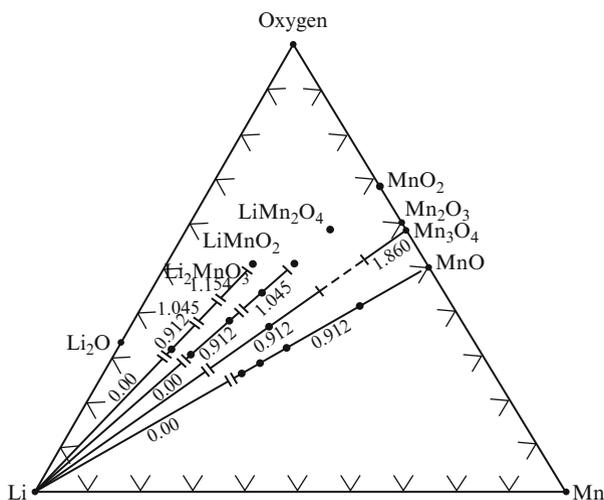

Fig. 12.26 Results of coulometric titration experiments on several phases in the Li-Mn-O ternary system. After [4]
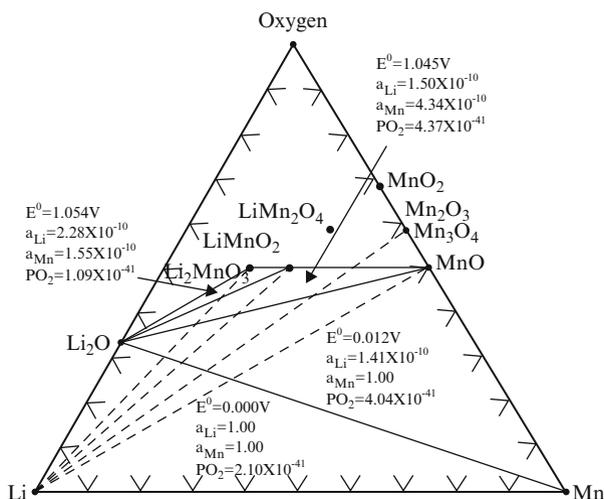

Fig. 12.27 Ternary phase stability diagram that resulted from the coulometric titration results shown in Fig. 12.26. After [4]

to the transition metal corner in this case. Instead, three of them lead to the composition Li_2O. Nevertheless, the principles and the experimental methods are the same.

It will be shown later, in Chap. 19, that some materials of this type behave quite differently at ambient temperature and higher potentials. In some cases lithium can be extracted from individual phases, which then act as insertion-extraction electrodes, with potentials that vary with the stoichiometry of individual phases. The principles involved in insertion-extraction reactions will be discussed later, in Chap. 13.

12.10   Ternary Systems Composed of Two Binary Metal Alloys

In addition to the ternary systems that involve a nonmetal component that have been discussed thus far in this chapter, it is also possible to have ternaries in which all three components are metals. Some such materials are possible candidates for use as reactants in the negative electrode of lithium battery systems.

One example will be briefly mentioned here, the Li-Cd-Sn system, which is composed of two binary lithium alloy systems, Li-Cd and Li-Sn. As will be described in Chap. 18, these, as well as a number of other binary metal alloy systems, have been investigated at ambient temperature. Their kinetic behavior is sufficiently fast that they can be used at these low temperatures. This system, as well as others, will be discussed in connection with the important mixed-conductor matrix concept.

12.10.1   An Example, the Li-Cd-Sn System at Ambient Temperature

If the two binary-phase diagrams and their related thermodynamic information are known, it is possible to predict the related ternary-phase stability diagram, assuming that no intermediate phases are stable. This assumption can be checked by making a relatively few experiments to measure the voltages of selected compositions. If they correspond to the predictions from the binary systems, there must be no additional internal phases. The value of this approach is that it gives a quick picture of what would happen if a third element were to be added as a dopant to a binary alloy.

As an example, the ternary-phase stability diagram that shows the potentials of all possible alloys in the Li-Cd and Li-Sn system [5] is shown in Fig. 12.28.
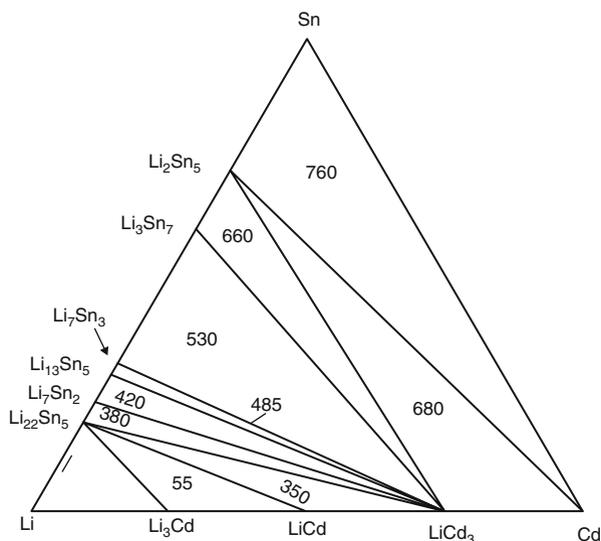
Fig. 12.28 Ternary phase stability diagram for the Li-Cd-Sn system. The numbers are the values of the voltage of all compositions in the various sub-triangles relative to pure lithium. After [5]

12.11 What About the Presence of Additional Components?

Practical materials often include additional elements, either as deliberately added dopants, or as impurities. If these elements are in solid solution in the major phases present in the ternary system, they can generally be considered to cause only minor deviations from the properties of the basic ternary system. Thus it is not generally necessary to consider systems with more than three components.

12.12 Summary

This rather long chapter has shown that the ideal electrochemical behavior of ternary systems, in which the components can be solids, liquids or gases, can be understood by the use of phase stability diagrams and theoretical electrochemical titration curves. The characteristics of phase stability diagrams can be determined from thermodynamic information, and from them the related theoretical electrochemical titration curves can be determined. Important properties, such as the maximum theoretical specific energy, can then be calculated from this information. A number of examples have been discussed that illustrate the range of application of this powerful method.

References

1. Luedecke CM, Deublein G, Huggins RA (1984) In: Veziroglu TN, Taylor JB (eds) Hydrogen Energy Progress V. Pergamon Press, New York, p 1421
2. Luedecke CM, Deublein G, Huggins RA (1985) J Electrochem Soc 132:52
3. Godshall NA, Raistrick ID, Huggins RA (1980) Mater Res Bull 15:561
4. Godshall NA, Raistrick ID, Huggins RA (1984) J Electrochem Soc 131:543
5. Anani AA, Crouch-Baker S, Huggins RA (1988) J Electrochem Soc 135:2103